

MMH Pyrolysis and Oxidation: Species Time-History Measurements behind Reflected Shock Waves

R. D. Cook, S. H. Pyun, D. F. Davidson, R. K. Hanson
Mechanical Engineering Department
Stanford University, Stanford CA USA

Abstract

Species time-histories were measured by laser absorption during monomethyl hydrazine (MMH) pyrolysis and oxidation behind reflected shock waves. Species measured included OH, NH₂, NH₃, CH₄, and MMH. Reflected shock conditions covered mixtures of 1% MMH in argon and 2.5% O₂ in argon ($\phi=1$) over a temperature range of 1000 to 1300 K and pressures near 2.6 atm. Measurements of OH and NH₂ were performed using narrow-linewidth laser absorption at 307 nm and 597 nm, respectively; NH₃ and MMH were measured using CO₂ laser absorption at 9.6 and 10.22 microns, respectively; and CH₄ was measured using DFB laser absorption at 3.4 microns. Measurements are compared to current MMH pyrolysis and oxidation kinetic mechanisms. Significant differences exist between the measurements and these models, much of which can be attributed to uncertainties in the rate constants and branching ratios for MMH decomposition.

1 Introduction

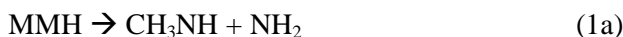
There is strong current interest in understanding the chemical kinetics of hypergolic propellants, both because of the need to improve modeling of rocket engines using these propellants and the need to improve understanding of the fundamental aspects of energetic material chemistry. Monomethyl hydrazine (MMH) is an established hypergolic propellant that is extensively used in rocket engines. However, very few shock tube studies of MMH pyrolysis or oxidation are available. Much of what is available is limited to ignition delay times and UV absorption profiles [1]. Thus, there is a critical need for high-quality species time-history and reaction rate constant measurements to test and refine detailed reaction mechanisms for MMH. Shock tube/laser absorption measurements can be used to generate this data.

We have recently developed a multi-wavelength shock tube/laser absorption scheme to provide species time-history data at high temperatures [2]. This method allows for the measurement of concentration time-histories of multiple species during high-temperature pyrolysis or oxidation using multiple laser probe beams to interrogate the test gas mixture behind a reflected shock wave. The advantages of this scheme are manifold. Shock tubes provide a near-ideal, constant-volume test reactor with test times up to tens of milliseconds (behind reflected shock waves), more than sufficient to study high temperature processes. They also provide well-established initial temperatures ($\pm 0.7\%$), pressures ($\pm 0.5\%$) and mixtures. Laser absorption diagnostics provide species-specific, sensitive (\sim ppm level),

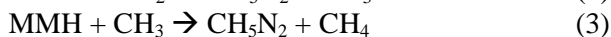
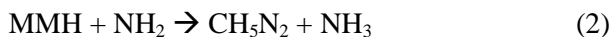
quantitatively accurate ($\pm 5\%$) detection of individual combustion species including reactants (in this study MMH), transient radicals (in this study, OH and NH_2) stable intermediates (in this study, NH_3 and CH_4), and products (e.g. H_2O and CO_2 , which however are not measured in this study).

Several detailed reaction mechanisms for MMH oxidation and pyrolysis exist. These include the ARO [3] and Catoire mechanisms [1] for oxidation, which are similar in the species profiles that they predict, and the Princeton mechanism [4] for pyrolysis. The Princeton mechanism has significantly different MMH decomposition pathways and rate constants and thus gives significantly different predictions for species profiles.

MMH has several possible decomposition pathways, but at high temperatures, decomposition is expected to be dominated by two major channels:



These two channels have similar bond dissociation strengths: 62.7 kcal/mol for formation of NH_2 and 64.7 kcal/mol for formation of CH_3 [4]. Measurements of the MMH decay rate can provide strong constraints on the overall rate constant for reaction (1), $k_{1a}+k_{1b}$. Immediate and subsequent reaction steps after the formation of these two radical intermediates lead to the formation of the stable intermediates NH_3 and CH_4 , in part, dominated during pyrolysis by the following two reactions:



Thus, measurements of NH_2 and CH_3 should, in theory, place constraints on the rate constants of the individual MMH decomposition channels (k_{1a} and k_{1b}) as well as on the competing removal reactions rates k_2 and k_3 . k_{1a} and k_{1b} should also be strongly related to the final yields of NH_3 and CH_4 during pyrolysis. Because of strong interferences from other species, laser absorption measurements of CH_3 at 216 nm (the strongest UV absorption feature accessible with current lasers) cannot be interpreted directly, and information about k_{1b} must in general be inferred from measurements of other species, e.g. CH_4 and MMH.

Here, using these shock tube/laser absorption methods, we investigate the decomposition pathways of MMH during pyrolysis and the role of transient radicals and intermediate species during oxidation and ignition. Species time-histories in both cases are compared to current mechanisms.

2 Shock Tube/Laser Absorption Facility

Measurements were performed in a large-inner-diameter (15.3 cm) high-purity stainless steel shock tube. Incident shock waves were generated by bursting polycarbonate diaphragms (0.25 mm thickness) against a fixed cutter using high-pressure helium. Incident shock speeds were determined using a series of five pressure transducers spread over the last meter of the driven section of the shock tube. Reflected shock conditions were calculated using the initial test gas composition and conditions, the incident shock speed extrapolated to the end wall, and the ideal shock equations assuming frozen chemistry.

Five species were measured: MMH, OH, NH_2 , NH_3 , and CH_4 . The OH, NH_2 and CH_4 laser absorption diagnostics were developed previously in our laboratory [2,5,6]. OH and NH_2 are measured at 597 and 307 nm respectively via visible or UV narrowline laser absorption using a ring dye laser. These diagnostics provide ppm sensitivity at high temperatures over the 15 cm pathlength and pressures near 2.6 atm. CH_4 is measured at 3.4 microns using a tunable DFG (difference frequency generation) diode laser. This diagnostic employs a scanned two-wavelength scheme to correct for broadband interference from larger alkanes.

NH_3 and MMH were measured (for the first time we believe in shock tubes) using a commercial CO_2 laser. MMH and NH_3 are measured at 10.22 and 9.6 microns, respectively, using selected single CO_2

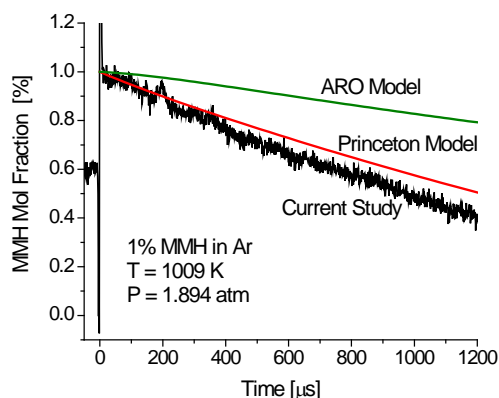
emission lines (e.g. P22 for MMH). The IR measurements of MMH and NH_3 are both free from broadband interferences that caused errors in previous UV measurements of these species. Concentrations were determined using Beer's law:

$$I_0/I = \exp(-k_\lambda P X L) \quad \text{Eqn. 1}$$

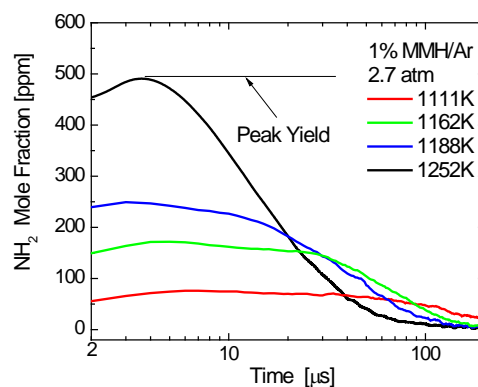
where I_0 and I are the measured incident and transmitted laser intensities, k_λ is the absorption coefficient at wavelength λ [$\text{atm}^{-1} \text{cm}^{-1}$], P is the total pressure [atm], X is the detected species mole fraction, and L is the test volume path length [cm]. I_0 and I were measured using a pair of matched TE-cooled MCT detectors.

3 MMH Pyrolysis

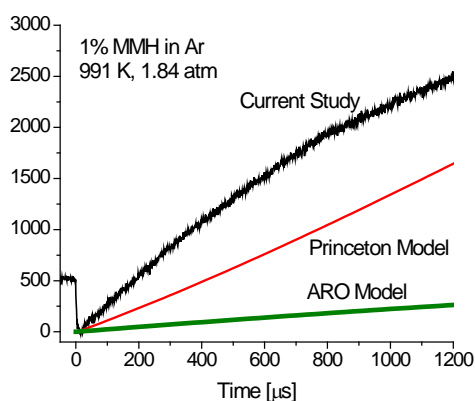
Figures 1-4 show example mole-fraction time-histories derived from laser absorption measurements of MMH, NH_2 , NH_3 and CH_4 and model simulations during MMH pyrolysis. The data exhibit excellent signal to noise ratio and rapid (MHz) time response. A comparison of the experimentally measured and model simulations for the NH_2 peak yields and the CH_4 plateau yields are shown in Figures 5 and 6.



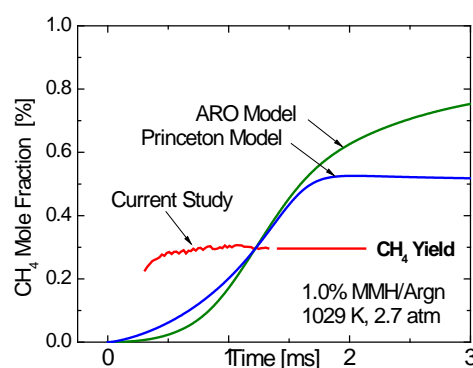
1



2

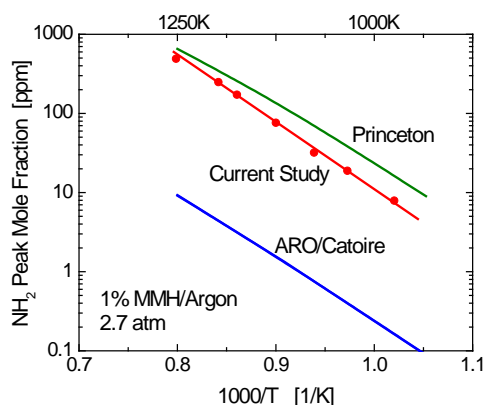


3

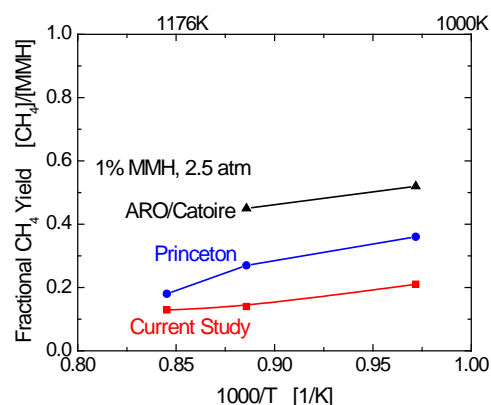


4

Figures 1-4. Species mole-fraction time-histories derived from laser absorption measurements during MMH pyrolysis. Constant-volume simulations using the ARO and Princeton mechanism are also shown. Simulation results for the Catoire model are similar to those of the ARO model.



5



6

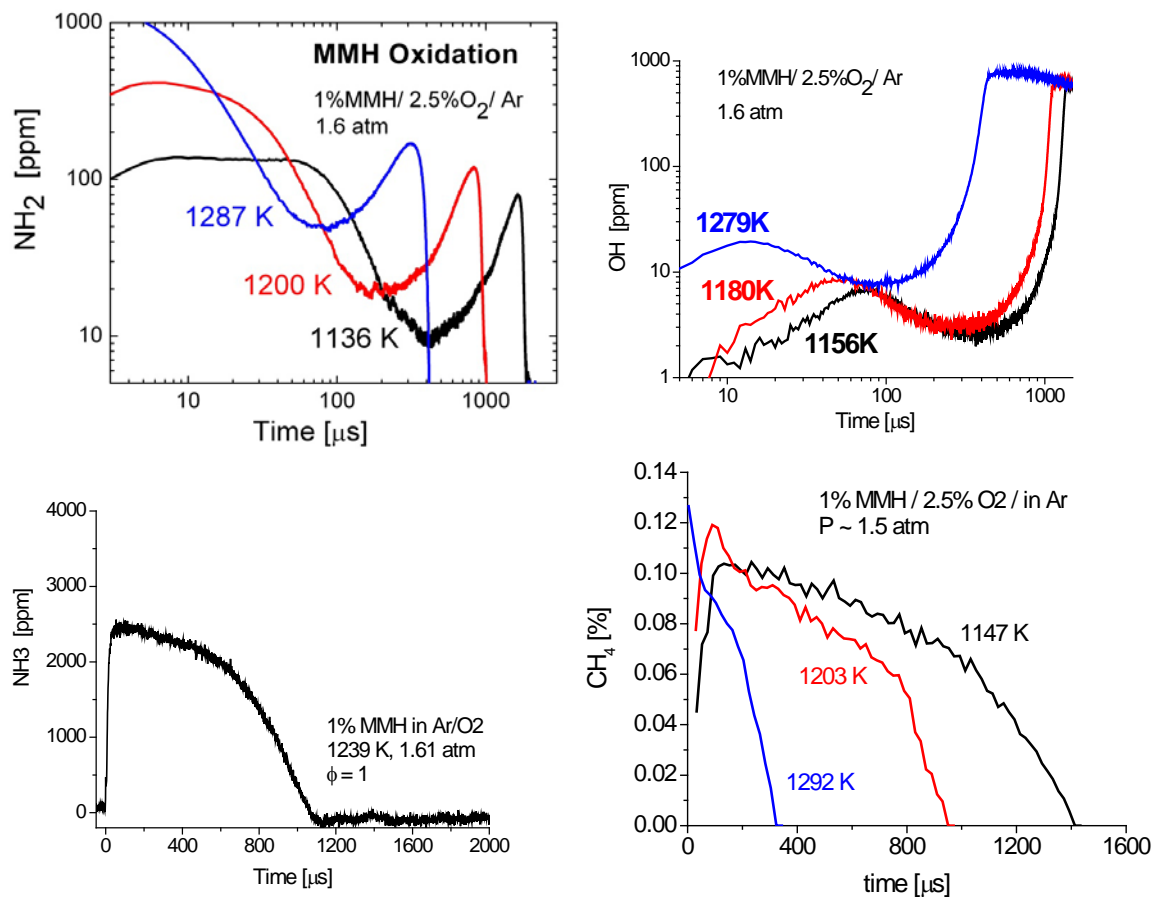
Figures 5 and 6. Comparison of the experimentally measured and model simulations for the NH_2 peak yields and the CH_4 plateau yields during MMH pyrolysis.

Figure 1 presents the first application of the new MMH IR laser absorption diagnostic. Relatively good agreement with the Princeton mechanism prediction for the overall removal rate of MMH is seen. Figures 2 and 5 presents the first shock tube measurements of NH_2 during MMH pyrolysis. Strong sensitivity of the peak NH_2 is seen with temperature. The comparison of the peak NH_2 yields to the predictions of the Princeton and ARO/Catoire mechanisms indicates that the Princeton simulations are more consistent with the data, but still are $1.3\text{--}2.3\times$ larger than measured values. Significant NH_2 yields imply high NH_3 yields. Figure 3 presents the first shock tube measurement of NH_3 during MMH pyrolysis using IR laser absorption. Large NH_3 yields (including conversions to NH_3 of greater than 25%) are seen at these conditions. Figures 4 and 6 shows that significantly smaller amounts of CH_4 are formed than existing models predict indicating the need to revise the value of k_{1b} in all three mechanisms.

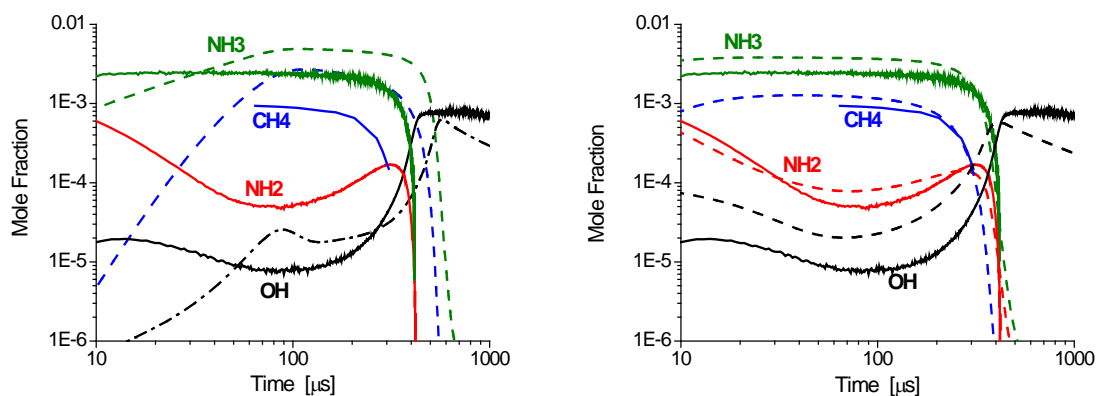
5 MMH Oxidation

Figures 7-10 show example species mole-fraction time-histories derived from laser absorption measurements of NH_2 , OH , NH_3 and CH_4 and model simulations during MMH oxidation. The NH_2 time-histories shown in Figure 7 provide data on multiple phases of oxidation. The early-time NH_2 yields provide constraints on the MMH decomposition pathway to NH_3 . The later formation of NH_2 provides a measure of the rate of NH_3 oxidation and the ignition delay time (for the overall system). Similarly, the OH time-histories shown in Figure 8 provide constraints on the role of radicals during the initial oxidation of MMH, the rapid rise of OH evident at later times is also a clear measure of the ignition delay time. The profiles of NH_3 and CH_4 shown in Figures 9 and 10 provide kinetic targets for modeling the oxidation rates of the two, likely most important, stable intermediate species that exist during the induction time before ignition.

Figure 11 show an overall comparison of the present species time-history measurements during MMH oxidation and a constant-volume simulation using the Catoire mechanism. Significant differences are seen in time scales of MMH decomposition and removal, and in the intermediate species profiles. Figure 12 shows a similar comparison with a modified version of the Catoire mechanism. In this mechanism, the MMH decomposition reactions and rate constants were replaced with those from the Princeton pyrolysis mechanism with only small changes. The Princeton rate constant for the rate constant for decomposition to NH_2 , k_{1a} , was multiplied by 0.5 and the decomposition of MMH to CH_3 , k_{1b} , was multiplied by 2. These preliminary changes demonstrate the significant effect that the MMH decomposition pathways and reaction rates can have on improving model simulations. Further work is needed to more comprehensively refine this mechanism.



Figures 7-10. Species mole-fraction time-histories derived from laser absorption measurements during MMH oxidation.



Figures 11-12. MMH oxidation: comparison of experiment and simulation. Initial reflected shock conditions : 1280 K, 1.5 atm, 1% MMH/ 2.5% O₂/ argon. Figure 11 presents simulations using the Catoire oxidation mechanism. Figure 12 presents simulations using the modified Catoire mechanism described in the text.

5 Conclusions

Shock tube/laser absorption measurements of concentration time-histories for five species were acquired during MMH pyrolysis and oxidation. These measurements provide the first dataset of MMH, OH, NH₂, NH₃ and CH₄ available for comparison with detailed MMH reaction models. Measurements of the reactant (MMH), one of the direct decomposition products (NH₂), and the two final pyrolysis products (NH₃ and CH₄) should provide modelers with the data needed to refine the values of the overall decomposition rate constant and branching ratios for MMH decomposition. These rate constants are critical to improving the performance of any detailed reaction mechanism for MMH. Using the results of the pyrolysis experiments, a simple refinement to the Catoire oxidation mechanism was performed with markedly successful results. Further improvements to both this oxidation reaction and the Princeton pyrolysis mechanism for MMH are now in progress. These methods should be directly applicable to the study of other hypergolic fuels. Studies of the “green” hypergolic fuel tetramethylethylenediamine (TEMEDA) are planned.

Acknowledgements

This work was sponsored by the Army Research Office / Multidisciplinary University Research Initiative (ARO/MURI), with Dr. Ralph A. Anthenien as contract monitor.

References

- [1] Catoire L, Bassin X, Dupre G, Paillard C. (1996). Shock Waves 6: 139.
- [2] Davidson DF, Hong Z, Pilla GL, Farooq A, Cook RD, Hanson RK. (2010). Multi-species time-history measurements during n-heptane oxidation behind reflected shock waves. Comb. Flame 157: 1899.
- [3] McQuaid MJ, Anderson WR, Kotlar AJ, Nusca MJ. Computational characterization of reactions employed to model monomethylhydrazine/inhibited red fuming nitric acid chemical kinetics. Proceedings of the 6th International Symposium on Special Topics in Chemical Propulsion (6-ISICP), 8-11 March 2005, Santiago, Chile.
- [4] Zhang P, Klippenstein SJ, Sun H, Law CK. (2010) Proc. Combust. Inst. 22 (*in press*).
- [5] Kohse-Höinghaus K, Davidson DF, Chang AY, Hanson RK. (1989). J. Quant. Spec. Radiat. Transfer 42:1.
- [6] Pyun SH, Cho J, Davidson DF, Hanson RK. (2010). Interference-free mid-IR laser absorption detection of methane. Measurement Sci. and Tech. (*submitted for publication*.)